Multimodality Imaging to Guide Ventricular Tachycardia Ablation in Patients with Non-ischaemic Cardiomyopathy

Ling Kuo,[1,2,3] Jackson J Liang,[3] Saman Nazarian[3] and Francis E Marchlinski[3]

1. Heart Rhythm Center, Division of Cardiology, Department of Medicine, Taipei Veterans General Hospital, Taipei, Taiwan; 2. Department of Medicine, National Yang-Ming University School of Medicine, Taipei, Taiwan; 3. Electrophysiology Section, Cardiovascular Division, Perelman School of Medicine, University of Pennsylvania, Philadelphia, PA, US

Abstract

Catheter ablation is an effective treatment option for ventricular tachycardia (VT) in patients with non-ischaemic cardiomyopathy (NICM). The heterogeneous nature of NICM aetiologies and VT substrate in patients with NICM play a role in long-term ablation outcomes in this population. Over the past decades, more precise identification of NICM aetiologies and better characterisation of various substrates have been made. Application of multimodal imaging has greatly contributed to the accurate diagnosis of NICM subtypes and improved VT ablation strategies. This article summarises the current knowledge of multimodal imaging used in the characterisation of non-ischaemic NICM substrates, procedural planning and image integration for the optimisation of VT ablation.

Keywords

Ventricular tachycardia, catheter ablation, non-ischaemic cardiomyopathy, late gadolinium enhancement, cardiac MRI, CT, PET, nuclear imaging

Disclosure: LK is supported by Taipei Veterans General Hospital-National Yang-Ming University Excellent Physician Scientists Cultivation Program, No 106-V-A-009. Additional support was provided by the Mark S Marchlinski Fund in Cardiac Electrophysiology. SN serves as PI for research funding from Biosense Webster, Imricor and Siemens, is a consultant to CardioSolv and is funded by US NIH NHLBI grants R01HL116280 and R01HL142893. FEM serves as consultant for Abbott Medical, Biosense Webster, Biotronik and Medtronic. The University of Pennsylvania Conflict of Interest Committee manages all commercial arrangements. JJL has no conflicts of interest to declare.

Received: 9 May 2019 **Accepted:** 19 September 2019 **Citation:** *Arrhythmia & Electrophysiology Review* 2019;8(4):255–64. **DOI:** https://doi.org/10.15420/aer.2019.37.3

Correspondence: Francis E Marchlinski, Electrophysiology Section, Cardiovascular Division, Perelman School of Medicine, University of Pennsylvania, 3400 Spruce St, Philadelphia, PA 19104, US. E: francis.marchlinski@uphs.upenn.edu

Catheter ablation has been increasingly used as a treatment for refractory ventricular tachycardia (VT) in patients with non-ischaemic cardiomyopathy (NICM). However, ablation outcomes tend to be quite variable because of the heterogeneity of the aetiology for the NICM and associated VT substrate in these patients.[1–3] Patients with NICM can be sub-classified based on specific genotypic and phenotypic findings, including dilated cardiomyopathy, arrhythmogenic right ventricular cardiomyopathy (ARVC), hypertrophic cardiomyopathy, restrictive cardiomyopathy, lamin A/C (LMNA) cardiomyopathy, sarcoid cardiomyopathy, amyloid cardiomyopathy, post-myocarditis cardiomyopathy and left ventricular (LV) non-compaction cardiomyopathy (LVNC).[4] While one recent multicentre study reported VT ablation outcomes of all NICM aetiologies, including myocarditis, sarcoidosis and valvular disease,[5] most VT ablation studies in NICM have focused on patients with the dilated cardiomyopathy phenotype and exclude patients with ARVC, hypertrophic cardiomyopathy, LVNC, restrictive cardiomyopathy, cardiac sarcoidosis (CS), valvular disease and acute myocarditis.[1,6,7]

The different NICM aetiologies exhibit discrete substrate patterns. Unlike the distinct dense scar, which exhibits subendocardial to transmural features in patients with prior MI and ischaemic cardiomyopathy (ICM), progression of myocardial fibrosis with predominantly perivalvular and/or intramural/subepicardial patterns is more commonly observed in NICM. This pattern of involvement can be demonstrated on cardiac MRI (CMR), electroanatomical voltage mapping (EAVM) and histology.[8–10]

Because of the presence of heterogeneous substrate in patients with different types of NICM, cardiac imaging is especially helpful to define the location and extent VT substrate and guide pre-procedural planning. This review will provide a summary of the current understanding of substrate characteristics identified by multimodal imaging and EAVM, the practicality of image integration during ablation procedures, as well as the impact of imaging modality utilisation on VT ablation outcome in various NICM aetiologies.

Value of Pre-procedural Imaging and Image Integration to Guide Refractory VT Ablation in Non-ischaemic Cardiomyopathy

Pre-procedural imaging is helpful to guide VT ablation in patients with healed MI and ICM. In these patients, multimodality imaging can help to identify arrhythmogenic substrate and critical components of VT circuits, leading to decreased radiofrequency ablation time, total procedure time, and improved acute and long-term ablation success rates.[11–17] In contrast, the impact of pre-procedural imaging to guide VT ablation in NICM differs based on the underlying NICM aetiology. Pre-procedural imaging can visualise the presence of epicardial substrates and predict when epicardial mapping may be

warranted.[18–20] Moreover, it localises important structures such as the phrenic nerve and epicardial coronary arteries which can be integrated into the electroanatomical map to avoid complications during ablation.[20,21]

CMR is the most well-studied imaging modality used to guide VT ablation in patients with NICM. Andreu et al. showed no difference in core scar detection between regular resolution (1.4–2.0 × 1.4–2.0 × 5.0 mm) and 3D high spatial resolution (1.4 × 1.4 × 1.4 mm) late gadolinium enhancement (LGE)-CMR, but more accurate characterisation of the border zone scar region using high spatial resolution CMR with thresholds set at 40–60% of maximal signal intensity (SI).[22] The border zone scar region on 3D LGE-CMR correlated with scar on EAVM in 79.2% of patients, compared with only 37.7–61.8% with 2D regular resolution CMR. However, there were only seven NICM patients in this 30-patient cohort referred for VT ablation.[22]

The feasibility of delineating small VT isthmuses on LGE-CMR in NICM requires further investigation. Siontis et al. compared acute and long-term ablation outcomes in idiopathic dilated cardiomyopathy (IDCM) patients with and without pre-procedural LGE-CMR and found that patients in whom pre-procedural LGE-CMR was performed and areas of possible VT substrate were defined, had higher acute procedural success (63% versus 24%; OR 7.86; p<0.001) and improved survival free of the composite endpoint of VT recurrence, heart transplantation or death (27% versus 60%; p=0.02).[23]

Cardiac CT imaging is another helpful imaging modality to guide NICM VT ablation. Esposito et al. identified arrhythmogenic substrate in 39 of 42 patients utilising CT with delayed enhancement.[24] Piers et al. integrated CT and LGE-CMR images simultaneously in 10 NICM patients and proposed an algorithm to detect epicardial and intramural arrhythmogenic substrate.[25] They found that in areas with fat thickness >2.8 mm, bipolar or unipolar voltage were attenuated and electrogram duration was lengthened, leading to failure of scar delineation from normal myocardium. In contrast, abnormal electrogram morphologies (late potentials, double potential, fragmented or >4 sharp spikes) could identify the substrate even with the existence of thick fat. In their study, a unipolar voltage cut-off value ≤7.95 mV was able to detect intramural scar. In a study by Yamashita et al., in which image-integration was used to guide VT ablation in 116 patients, 89% of critical VT isthmuses and 85% of local abnormal ventricular activities (LAVA) sites could be identified.[21] The efficiency in identifying LAVA with imaging was higher in ICM (90%) and ARVC (90%) than in NICM (72%).

Figure 1 shows an LV wall thickness shell with reconstruction of the aorta, coronary arteries and septal aneurysm generated from CT. *Figure 2* shows a pre-procedural LGE-CMR image depicting anteroseptal patchy scar and inferolateral transmural scar. Registration of the CMR-segmented LV shell to endocardial and epicardial EAVM by using landmarks of aorta, LV apex and mitral annulus is successfully accomplished.

Pre-procedural images can be segmented and displayed as 3D shells and integrated into the electroanatomical map for intraprocedural use. Since critical VT circuits can be quite small, accurate registration of the CT or CMR-segmented 3D models with the EAVMs is crucial to permit precise evaluation of structural as well as electrical abnormalities. Utilisation of intracardiac echo for identification of the cusps and true LV/right ventricle (RV) apices, and their use as landmarks can be extremely helpful for accurate image registration at the time of the procedure. The landmarks and registration distances between CMR or CT-segmented images and electroanatomical maps as well as their impact on outcome in different studies are summarised in *Table 1*.

VT Substrate Patterns in Different Non-ischaemic Cardiomyopathy Aetiologies

Idiopathic Dilated Cardiomyopathy

There are two predominant substrate patterns in patients with IDCM as identified by unipolar voltage on EAVM and LGE-CMR.[26–28] the first is a basal, anteroseptal scar pattern, which frequently extends to the perivalvular region, as well as subepicardial, and the second is an inferolateral or true posterior scar pattern. Identifying the scar pattern in IDCM with pre-procedural imaging allows one to anticipate acute and long-term ablation success, and provide valuable information to share with patients prior to their procedure.

While acute ablation success rates are similar between these two scar patterns, patients with anteroseptal as opposed to inferolateral scar pattern are more likely to have long-term VT recurrence and require repeat ablation.[27] In addition, the anteroseptal scar pattern often predicts VT circuit location near the conduction system, prompting pre-procedural discussion about the possibility of atrioventricular block and need for permanent pacing strategies. Frequently, anteroseptal scar patterns extend to involve extensive areas of the endocardial and epicardial perivalvular LV.

Oloriz et al. have previously characterised electrogram abnormalities correlating with CMR substrate and reported that late potentials were more frequently seen on the epicardium in patients with an inferolateral (80%) versus anteroseptal (7%) scar pattern.[27] Differences in ablation success between these two groups are likely to be a result of difficulties in targeting VT substrate in the anteroseptal group, as well as the higher prevalence of septal hypertrophy. While patients with inferolateral substrate are more likely to have epicardial late potentials that may be amenable to ablation from the epicardium or coronary venous system, those with anteroseptal substrate frequently have deep intramyocardial substrate within the interventricular septum or LV summit, where effective energy delivery and substrate elimination is difficult with currently available tools.

Our group have also reported a strong association between electrogram characteristics and the transmural extent and intramural types (endocardial, mid-wall, epicardial, patchytransmural) of scar as measured on LGE-CMR in IDCM. Myocardial wall thickness, scar transmurality, and intramural scar types were independently associated with electrogram amplitude, duration, and deflections. Fractionated and isolated potentials were more likely to be observed in regions with higher scar transmurality (p<0.0001 by ANOVA) and in regions with patchy scar (versus endocardial, mid-wall, epicardial scar; p<0.05 by ANOVA). Most VT circuit sites were located in scar with >25% scar transmurality.[18]

Figure 3 shows a patient with NICM in whom VT was terminated with ablation at a site from LV endocardium that correlated with intramural scar identified by low unipolar voltage of EAVM and LGE-CMR.

In addition to LGE-CMR, fludeoxyglucose (FDG)-PET imaging holds promise for dissecting the role of active inflammation in NICM VT patients.

Figure 1: Left Ventricular Wall Thickness Shell with Reconstruction of the Aorta, Coronary Arteries and Septal Aneurysm Generated from CT

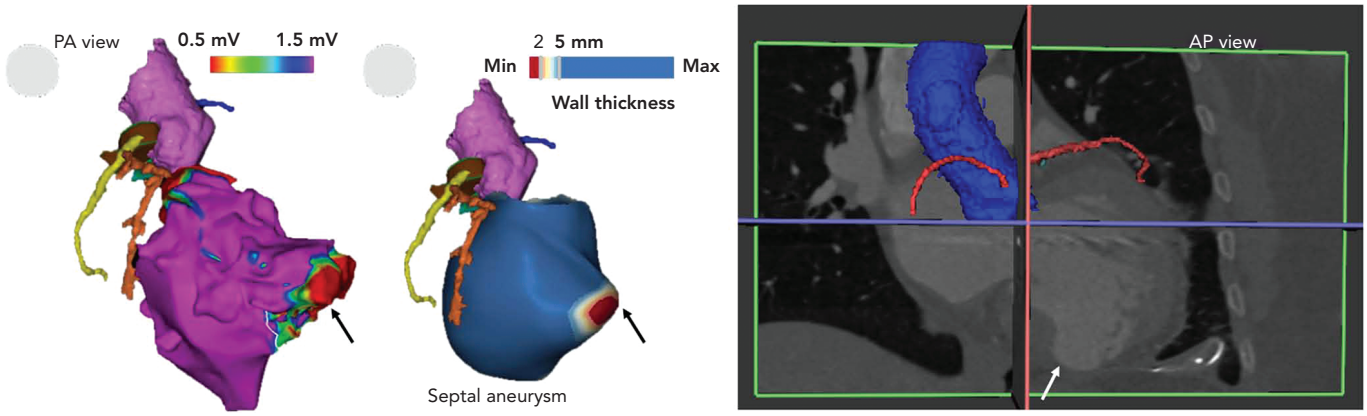

The 3D left ventricle shell, aorta, coronary arteries and septal aneurysm (arrow) are generated from CT imaging. Wall thickness of the left ventricle can be displayed, which defines wall thinning <5 mm as abnormal according to previous ischaemic cardiomyopathy scar. AP = anteroposterior; PA = posteroanterior.

Figure 2: Pre-procedural Late Gadolinium Enhancement-Cardiac MRI Depicting Anteroseptal Patchy Scar and Inferolateral Transmural Scar

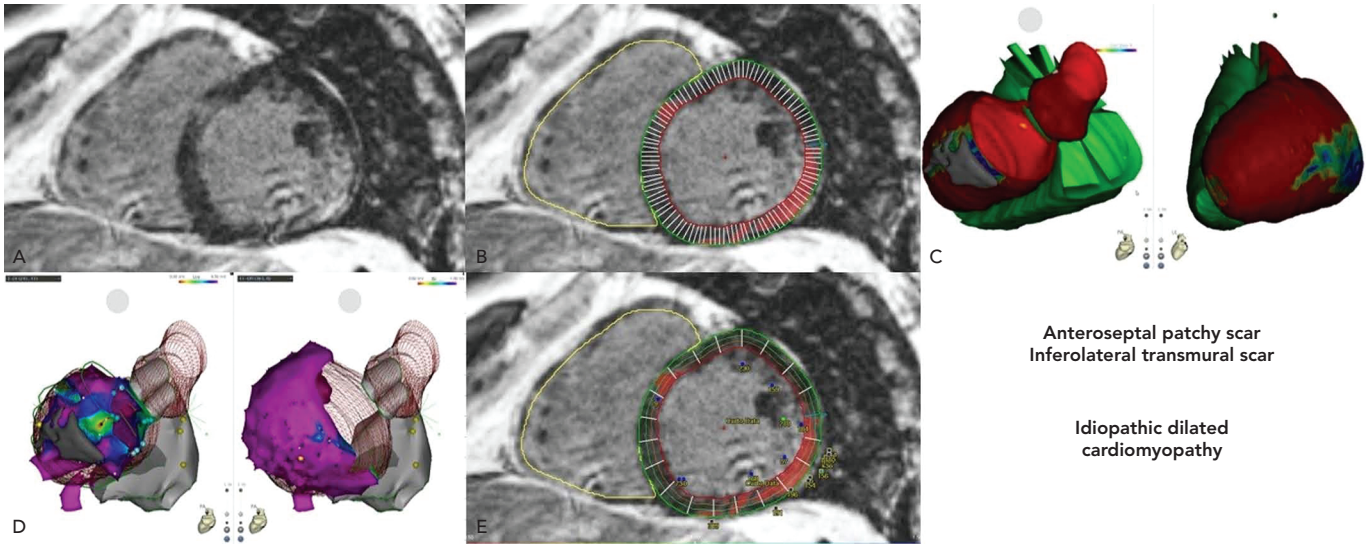

A: Anteroseptal patchy scar and inferolateral transmural scar on late gadolinium enhancement-cardiac MRI (CMR); B: Endocardial and epicardial contouring of the left ventricle (LV) and scar detection based on 6 standard deviations from remote normal myocardium; C: 3D right ventricle, LV endocardial and epicardial shell generated from CMR; D: Registration of electroanatomical voltage mapping and CMR-segmented LV shell utilising Carto Merge module by using landmarks of aorta, mitral annulus and LV apex; E: Electroanatomical voltage mapping points projected to late gadolinium enhancement-CMR can associate electrograms with signal intensity based on CMR. Courtesy of Dr Jae-Seok Park, Electrophysiology, Division of Cardiology, Department of Medicine, Mediplex Sejong General Hospital, South Korea.

Tung et al. showed that nearly half of patients referred with unexplained cardiomyopathy and ventricular arrhythmia have focal myocardial inflammation on PET, suggesting an occult arrhythmogenic inflammatory cardiomyopathy in these 'idiopathic' NICM patients.[29] The potential benefit of immunosuppressive medical therapy is unclear. One review suggested that identification of arrhythmogenic inflammatory cardiomyopathy, may prompt the usage of the anti-inflammatory medical therapy in early stage of arrhythmia before catheter ablation.[30] Further efforts on establishing optimal diagnostic and treatment paradigms for NICM VT and premature ventricular contraction patients are warranted.

Cardiac Sarcoidosis

Cardiac sarcoidosis (CS) is an under-diagnosed aetiology of NICM. Cardiac imaging modalities, including LGE-CMR and PET, have dramatically improved the diagnosis of CS and can define the substrate in patients undergoing VT ablation.[31–33] The distribution of LGE in patients with CS is variable and frequently patchy, often involving the interventricular septum (predominantly involving the basal and/or mid-ventricular septum, with or without RV involvement) and inferolateral wall.[34,35] Additionally, LGE is more frequently seen in subepicardial layers.[36]

Muser et al. reported that approximately one-third of all affected cardiac segments revealed transmural LGE with preserved wall thickness in patients with CS and VT undergoing ablation.[37] The presence of LGE on CMR identifies areas with inflammation, granuloma and scar on necropsy.[38,39]

Interestingly, compared to patients with IDCM, those with CS tend to have more abnormal electrograms.[37] Whether fibrosis or active inflammation represents the main culprit contributing to

Table 1: Studies of Non-ischaemic Cardiomyopathy Ventricular Tachycardia Ablation with Image Integration Using Pre-procedural CT and Cardiac MRI Images

Studies	Patient Population	Image Modalities and Resolution (mm)	EAVM and Mapping Catheter	Registration Method	Registration Accuracy (mm)	Anatomical Landmark	Outcome
Bogun et al. 2009[19]	NICM (n=29)	CMR: 1.4 × 2.2 × 8.0	Carto 3.5 mm catheter	Landmark + surface; CartoMerge	4.8 ± 3.6	Aorta, LV apex, mitral annulus	Identify arrhythmogenic substrate in NICM and strategy
Spears et al. 2012[87]	NICM (n=10)	CMR: 1.3 × 1.3 × 6.0	Carto 3.5 mm catheter	Landmark + surface; CartoMerge	3.6 ± 2.9	Aorta, His bundle, mitral valve annulus, LV apex	BV >1.9 mV and UV <6.7 mV had a NPV of 91% for detecting non-endocardial scar from no scar or endocardial scar
Cochet et al. 2013[62]	ICM (n=3) NICM (n=3) Myocarditis (n=2) IDCM (n=1)	CMR: 1.25 × 1.25 × 2.5	Carto and NavX, PentaRay and 3.5 mm catheter	Landmark + surface; CartoMerge	N/R	Coronary sinus, aortic root, left atrium, LV, mitral annulus	In myocarditis, sub-epicardial LGE matched areas of epicardial low voltage.
Desjardins et al. 2013[60]	NICM (n=15) • 11: IDCM • 4: sarcoidosis	CMR: 1.4 × 2.2 × 8.0	Carto 3.5 mm catheter or 4 mm catheter	Landmark + surface; CartoMerge	<5.0	Aorta, mitral annulus, LV apex	Define best cutoff values of BV <1.55 mV and UV <6.78 mV to separate endocardial measurements overlying scar as compared with areas not overlying a scar.
Piers et al. 2013[25]	NICM (n=10)	CMR: N/R CT: 0.5 × 0.5 × 2.0	Carto 3.5 mm catheter	Landmark + visual alignment; CartoMerge	3.2 ± 0.4	Left main coronary artery	BV, UV and electrogram duration >50 ms Can distinguish scar from normal myocardium in areas <2.8 mm fat
Piers et al. 2014.[7]	ICM (n=23) NICM (n=21)	CMR: N/R	Carto 3.5 mm catheter	Landmark + visual alignment; CartoMerge	3.8 ± 0.6	Left main coronary artery	Critical isthmus sites located in close proximity to CMR-derived core-border zone transition and in regions with >75% transmural scar
Yamashita et al. 2016[21]	NICM (n=30) ARVC (n=19)	CMR: 1.25 × 1.25 × 2.5; CT angiography: thickness 0.6	Carto and NavX, multielectrode (1-2-1 mm) or 4 mm catheter	Landmark + surface; CartoMerge or field scaling of NavX	3.9 ± 1.0	N/R	Integration motivated additional mapping; 43% modified epicardial ablation strategy owing to the localisation of vessels and nerve
Esposito et al. 2016[24]	NICM (n=19) • 12: IDCM • 1: LMNA • 5: myocarditis • 1: other	CT: N/R	Carto: N/R	Landmark + surface; CartoMerge	2.9 ± 2.1	Aorta, LV	Delayed enhancement segments on CT correlated with low voltage area

ARVC = arrhythmogenic right ventricular cardiomyopathy; BV = bipolar voltage; CMR = cardiac magnetic resonance; EAVM = electroanatomical voltage mapping; ICM = ischaemic cardiomyopathy; IDCM = idiopathic dilated cardiomyopathy; LGE = late gadolinium enhancement; LMNA = lamin A/C; LV = left ventricle; N/R = not reported; NICM = non-ischaemic cardiomyopathy; NPV = negative predictive value; UV = unipolar voltage.

sustained monomorphic VT remains unclear.[37,40,41] Blankstein et al. demonstrated that the presence of focal perfusion defects with ^{82}rubidium nuclear scanning and FDG uptake on cardiac PET identified patients at higher risk of VT or death.[40] In contrast, Muser et al. found that the abnormal electrograms were more correlated with LGE on CMR rather than inflammation identified by PET.[37] *Figure 4* shows an example of fractionated electrograms located in the LGE region on CMR, with good pace-mapping QRS morphology similar to clinical VT morphology.

While there is no definite benefit of immunosuppressive therapy in patients with monomorphic VT and NICM, this strategy is a reasonable approach in patients with CS and VT, particularly in the acute inflammatory phase of the disease when polymorphic VT may be manifest. VT characteristics and ablation outcomes can differ based on the degree of active inflammation with CS, and VT ablation outcomes in patients with CS tends to be worse than other aetiologies of NICM.[1,5,42]

Lamin A/C Cardiomyopathy

LMNA cardiomyopathy can present in a similar manner to CS, with conduction abnormalities, ventricular arrhythmias and heart failure. The diagnosis can be confirmed with advanced genetic testing.

Consideration of the diagnosis of LMNA cardiomyopathy should be made in all patients with suspected CS who do not respond to anti-inflammatory treatment or who do not have evidence of active inflammation on PET imaging. The specific substrate pattern in LMNA cardiomyopathy, as characterised by CMR, predominantly involves the basal and anteroseptal segments with preserved wall thickness.

Figure 3: Example of the Association Between Double Potential with Intramural Late Gadolinium Enhancement and Termination of Ventricular Tachycardia

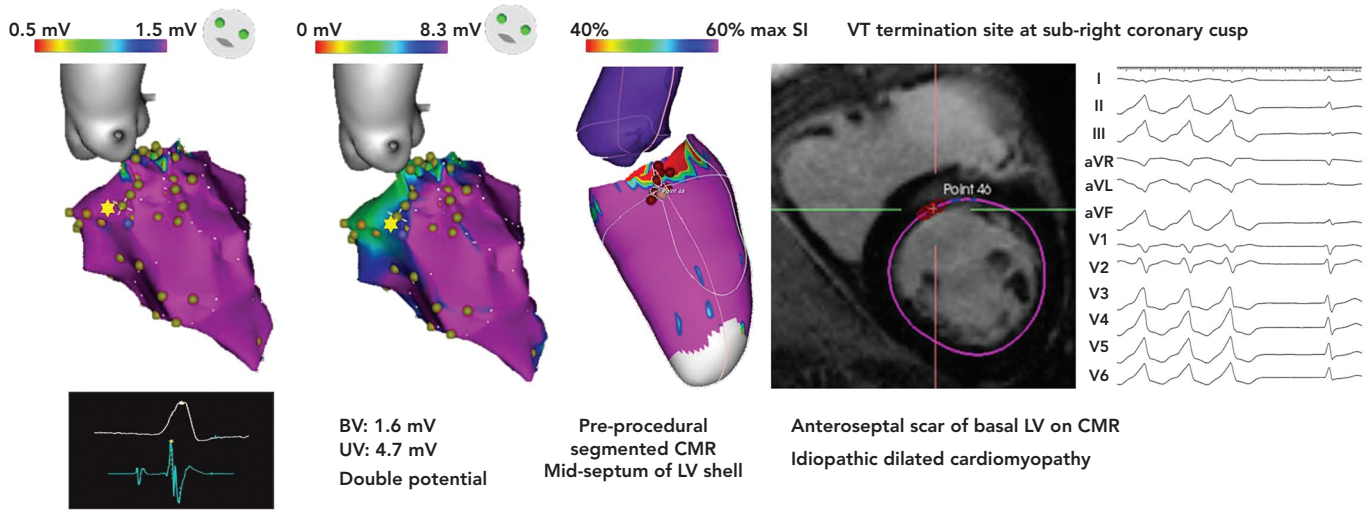

Normal bipolar voltage but abnormal unipolar voltage around the perivalvular area extending to anteroseptal wall are noted on electroanatomical voltage mapping (EAVM). Pre-procedural late gadolinium enhancement (LGE)-CMR segmented LV shell displays perivalvular to anteroseptal scar involving mid-septum. After registration of EAVM and LGE-segmented LV shell, the VT termination point on EAVM is projected to LGE region on CMR. BV = bipolar voltage; CMR = cardiac magnetic resonance; LV = left ventricle; RV = right ventricle; SI = signal intensity; UV = unipolar voltage; VT = ventricular tachycardia.

Figure 4: Example of Fractionated Electrograms Located in the Late Gadolinium Enhancement Region on Cardiac MRI

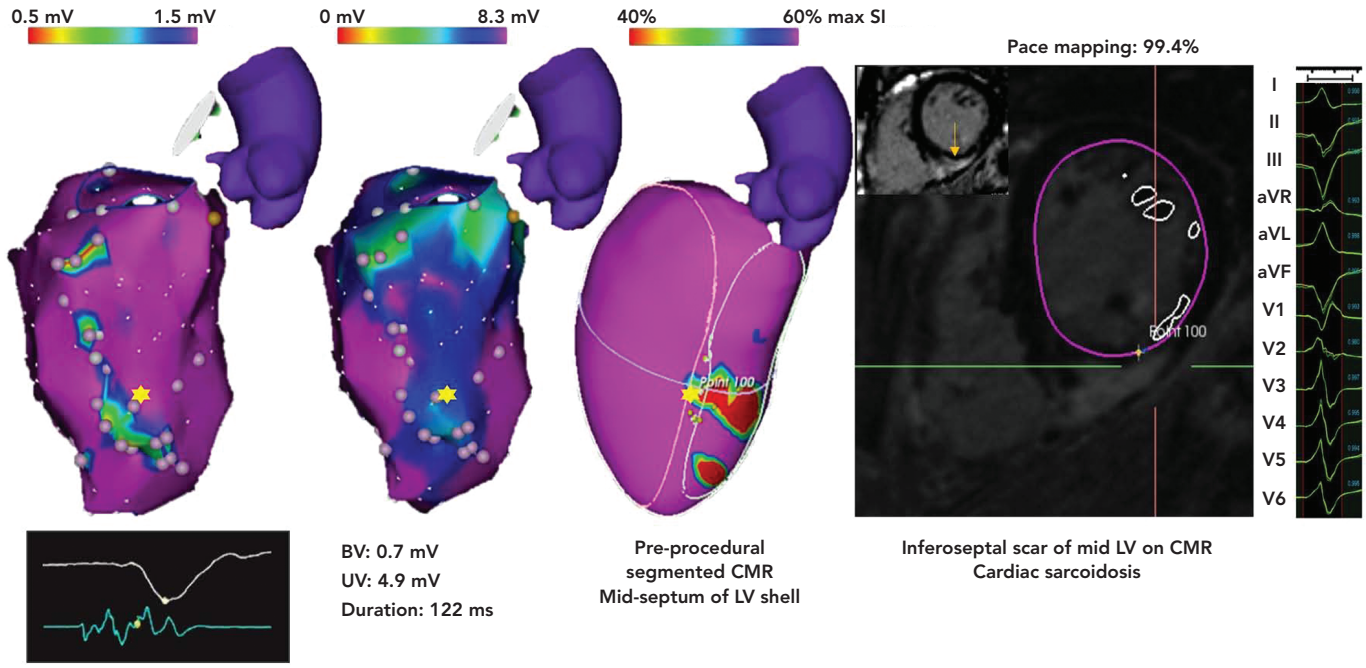

Small area of abnormal bipolar voltage at septum of mid-LV and extensive abnormal unipolar voltage from basal, perivalvular, inferoseptal wall to mid-LV are noted on electroanatomical voltage mapping. Pre-procedural late gadolinium enhancement-CMR segmented LV shell displays inferoseptal scar at mid-septum of mid LV. The good pace-mapping point on electroanatomical voltage mapping is projected to late gadolinium enhancement region on CMR. BV = bipolar voltage; CMR = cardiac magnetic resonance; LV = left ventricle; SI = signal intensity; UV = unipolar voltage.

Importantly, VT ablation outcomes in patients with LMNA cardiomyopathy tend to be among the worst of all NICM subgroups.[43,44]

One study reported a dismal 25% success rate despite multiple ablations, and frequently requiring supplementary techniques such as ethanol injection or surgical ablation. Furthermore, nearly all (91%) patients had ≥1 VT recurrence after the last procedure, and the disease process tended to rapidly progress, with a mortality rate of 26% of patients, and a high rate of heart transplantation because of end-stage heart failure.[44] Reasons for poor success with VT ablation in patients with LMNA cardiomyopathy include poor accessibility of the substrate which tends to be basal septal and intramural.

Myocarditis

Myocarditis is an important cause of dilated cardiomyopathy worldwide. LGE-CMR and T2-weighted sequences are useful imaging methods for diagnosis of myocarditis.[45] The pattern of VT substrate in patients with post myocarditis cardiomyopathy typically involves the sub-epicardium

and lateral basal LV, and a combined endocardial and epicardial approach is frequently necessary to achieve durable VT elimination.[46,47] A recent multicentre study of 50 patients with myocarditis-related VT reported 1-year VT recurrence rate of 23%.[5]

Left Ventricular Non-compaction

LVNC is a rare genetic cardiomyopathy, which results from the cessation of embryogenesis of endocardium and mesocardium, generating two-layered structure of the myocardium with a compacted, thin epicardial layer and a non-compacted, thickened endocardial layer with deep intertrabecular recesses. This process mostly affects the inferior and lateral wall from mid to apical LV.[48–51] Muser et al. showed that areas with abnormal electroanatomical substrates and low bipolar voltage in patients with VT and LVNC correlate well with non-compacted segments seen on CMR or echocardiography in the majority (75%) of patients.[52] Wan et al. found that LGE was detected on CMR in 19 of 57 patients with LVNC, with variable distribution and frequently involving the septum.[53] The mechanisms by which LGE develops in patients with LVNC are not understood.

Arrhythmogenic Right Ventricular Cardiomyopathy

ARVC is an inherited cardiomyopathy, which is characterised by cardiac myocyte degeneration and fibro-fatty replacement. Akdis et al. suggested that typical ARVC is the right-dominant subtype of arrhythmogenic cardiomyopathy, which is predominantly associated with mutations in genes encoding proteins of the intercalated disc.[54] The other two subtypes, including biventricular form and left-dominant form, are mimics of other NICM including sarcoidosis. ARVC can also occur without evidence of desmosomal protein abnormalities suggesting a predominant role for a triggering mechanism and not a genetically determined degenerative disease.

The exact triggering mechanism for disease manifestation and progression is poorly understood but the absence of rapid scar progression appears to be the rule rather than the exception.[55] Fibro-fatty tissue infiltration typically extends from the epicardial surface or mid-myocardium, and may involve the entire thickness of the myocardium.[56] CT can identify arrhythmogenic substrate for ARVC patients. Komatsu et al. demonstrated that the majority of LAVAs were located in segments with extensive intramyocardial fat (80%).[57] Yamashita et al. also demonstrated a 90% agreement between LAVAs and hypo-attenuated areas identified on multi-detector CT.[21]

Correlation Between Substrate Derived with Electroanatomical Voltage Mapping and Cardiac MRI/CT/PET

Prior electroanatomical voltage mapping studies have defined normal endocardial and epicardial bipolar voltage cut-offs of >1.5 mV and >1 mV, respectively, and normal unipolar voltage cutoff of >8.3 mV.[58,59]

Different voltage cut-off values have been proposed to identify scar based on correlation with multimodality imaging. Desjardins et al. evaluated 11 IDCM and four sarcoidosis patients with intramural scar detected on LGE-CMR utilising full width at half maximum (FWHM) method, and identified bipolar and unipolar voltage cut-offs of 1.55 mV and 6.78 mV, respectively, to define intramural scar.[60]

Meanwhile, Liang, et al. identified a unipolar voltage cut-off of 4.8 mV to best correlate with interventricular septal scar defined by FWHM on CMRI in patients with IDCM and VT but noted that VT electrogram substrate and origin of VT can occur in approximately 10–20% of patients in the absence of LGE in regions with low unipolar voltage using the higher cut-off value of 8.3 mV.[61]

In a series that included 15 patients (10 with IDCM and five with CS), we determined that voltage thresholds of 1.78 mV and 5.64 mV for bipolar and unipolar scar, respectively, maximise both sensitivity and specificity for identification of LGE on CMR.[18] Piers, et al. identified LV endocardial bipolar and unipolar voltage cut-offs of 2.04 mV and 9.84 mV to define scar correlating with LGE-CMR (modified FWHM, ternary method set SI thresholds at 35% and 50% of maximal SI).[28] During epicardial voltage mapping, Piers et al. identified bipolar and unipolar voltage cut-offs of 1.81 mV and 7.95 mV, respectively, to correlate with LGE-CMR in 10 NICM patients with VT.[25]

Maccabelli et al. showed that 95% of patients with myocarditis-related VT had subepicardial LGE on CMR that correlated with areas of unipolar voltage <8 mV.[46] Of note, the above-mentioned studies utilised a 3.5 mm tip open-irrigated catheter with 2 mm ring electrode and 1 mm inter-electrode spacing, or a solid-tip 4 mm catheter for EAVM sampling. Importantly, the validity of different voltage cut-off values for defining abnormal substrate should be confirmed/established for maps created using catheters with different interelectrode spacing and specifically when using small electrode size recording tools.

The utility of CT imaging to define VT substrate in patients with NICM has been less well defined. In a small study of 12 patients with IDCM, Esposito et al. demonstrated good correlation between CT-defined substrate (wall thinning <5 mm on CT angiography or visually defined enhanced segments on delayed-enhanced CT) with areas of bipolar and unipolar scar detected with EAVM.[24]

Cochet et al. acquired high-density endocardial and epicardial EAVM and registered to CMR/multi-detector CT, and found that LGE on CMR and wall-thinning <5 mm at CT corresponded to low voltage areas with bipolar voltage <1.5 mV and LAVA.[62] On the contrary, Yamashita et al. demonstrated a poor correlation between wall thinning and EAVM scar (13 ± 16% agreement) in 28 NICM patients with multi-detector CT imaging.[21]

To date, no studies have investigated the correlation between the substrate on EAVM and LGE on CMR or delayed perfusion area on CT in hypertrophic cardiomyopathy patients, and the effect of ventricular hypertrophy on scar voltage cut-offs with EAVM remains unclear. Bazan et al. demonstrated that the myocardial wall thickness or distance from the normal tissue to the abnormal substrate is one of the key factors that can influence the interpretation of abnormal unipolar voltage cut-off value.[63] In patients with hypertrophy, the applicable unipolar cut-off value when using a 3.5 mm electrode tip may be greater than the standard 8.3 mV cut-off.[64,65]

Titrating the slider bar up to 10 mV, or even higher, in the setting of LV hypertrophy may permit identification of areas with layered mid-myocardial or epicardial scar. Glashan et al. confirmed the linear association of wall thickness with both unipolar or bipolar voltage in the myocardium without fibrosis detected by histology.[66] In these scenarios, certain regions that 'ghost in' when adjusting the slider bar upwards may represent areas of intramural and epicardial substrate in patients with LV hypertrophy.

Table 2: The Identification of Arrhythmogenic Substrate by Different Image Modalities

Studies	Patient Population	Image Modalities	Multimodal Imaging Substrate	Electroanatomical Substrate	Correlation of Images and Electroanatomical Substrate
Dickfeld et al. 2008[88]	ICM (n=12) NICM (n=2)	PET-CT Thallium scan or rubidium PET	Scar: FDG to blood flow match pattern Diseased/hibernating myocardium: FDG to blood flow mismatch pattern	BV <0.5 mV: scar; 0.5–1.5 mV: abnormal myocardium	PET/CT-derived scar maps correlate with voltage map (r=0.89; p<0.05) Scar size, location and border zone predict high resolution voltage map channels (r=0.87; p<0.05).
Bogun et al. 2009[19]	NICM (n=29)	CMR	Two blinded observers identify LV scar and manually contoured for quantification	BV <1.5 mV: scar (LVA)	CMR-derived scar size correlates with endocardial scar size (BV <1 mV: r=0.96; p<0.0001; BV <1.5mV: r=0.94, p<0.0001)
Santangeli et al. 2011[69]	ARVC (n=18) Myocarditis (n=13) Idiopathic RV outflow tract (n=5)	CMR	Experienced radiologist blindly identifies RV scar	BV <0.5 mV: scar; 0.5–1.5 mV: border zone	Scar ≥20% of the RV area is the best cutoff value to detect LGE (Sen: 83%, Spe: 92%)
Spears et al. 2012[87]	NICM (n=10)	CMR	Core scar: SI ≥50% of maximal myocardial SI Grey scar: SI > the maximum remote myocardial SI, but <50% of the maximal SI (full width at half-maximum)	N/R	BV >1.9 mV and UV <6.7 mV: 91% NPV for detecting non-endocardial scar from no scar or endocardial scar
Cochet et al. 2013[62]	ICM (n=3) NICM (n=3) Myocarditis (n=2) IDCM (n=1)	CMR CT	Scar: 50–100% of maximal myocardial SI Grey zone: 35–50% of maximal myocardial SI Wall-thinning: LV end-diastolic wall thickness <5 mm	BV <1.5 mV as LVA and LAVA	NICM: poor overlap of LGE CMR-defined substrate with EAVM LVA Wall-thinning matched areas of LVA with an overlap of 63 ± 21% Myocarditis: good overlap of sub-epicardial LGE with LVA (scar: 83 ± 24%; grey zone: 92 ± 12%) Wall-thinning was not found despite the presence of LV epicardial low voltage.
Desjardins et al. 2013[60]	NICM (n=15)	CMR	Two blinded observers identified scar	BV <1.5 mV: LVA	1.55 mV for BV (AUC=0.69, Sen: 61%, Spe: 66%) and 6.78 mV for UV (AUC=0.78, Sen: 76%, Spe: 69%) are best cutoff values for the identification of intramural substrate
Piers et al. 2013[25]	NICM (n=10)	CMR CT	Scar: >35% maximal myocardial SI Fat thickness	BV <1.5 mV: LVA	1.81 mV for BV (AUC: 0.73, Sen: 59%, Spe: 78%) and 7.95 mV for UV (AUC: 0.79, Sen: 80%, Spe: 72%) enables to distinguish scar from normal myocardium in areas <2.8 mm fat
Esposito et al. 2016[24]	NICM (n=19)	CT	Visually defined delayed enhanced segments as scar and the scar transmurality	BV ≤1.5 mV UV ≤8 mV (for LV) Late potentials	Delayed enhancement segments on CT correlated with low voltage area (Sen: 76%, Spe: 86%, NPV: 95%)
Liang et al. 2018[61]	NICM (n=95)	CMR	Scar: full width at half-maximum method	BV ≤1.5 mV UV ≤8.3 mV	4.8 mV for UV cutoff value provides best correlation with LGE on CMR (AUC: 0.75, Sen: 75%, Spe: 70%)
Xie et al. 2018[70]	ARVC (n=10)	CMR	N/R	Epicardium: BV ≤0.5 mV: dense scar BV >1 mV: normal myocardium	SI Z score >0.05 correlates with BV <0.5 mV and <–0.16 correlates with BV >1 mV SI Z score >0.05 identifies delayed potentials in the RV epicardium (Sen: 72%, Spe: 56%)

ARVC = arrhythmogenic right ventricular cardiomyopathy; BV = bipolar voltage; CMR = cardiac MRI; FDG = fludeoxyglucose; ICM = ischaemic cardiomyopathy; IDCM = idiopathic dilated cardiomyopathy; LAVA = local abnormal ventricular activities; LGE = late gadolinium enhancement; LV = left ventricle; LVA = low-voltage area; N/R = not reported; NICM = non-ischaemic cardiomyopathy; NPV = negative predictive value; RV = right ventricle; Sen = Sensitivity; SI = signal intensity; Spe = Specificity; UV = unipolar voltage.

Several important issues must be considered when evaluating RV substrate. First, the RV free wall is thin and normal voltage cut-offs differ from the RV septum. Second, the aortic root, which overlaps the RV septum to RV outflow tract (RVOT), can influence the normal voltage cut-off. Finally, in addition to scar, fat can be arrhythmogenic in patients with ARVC.

Normal RV endocardial voltage cut-offs, based on studies examining patients with normal ventricles without evidence of EAVM or CMRI scar, have been identified to be >1.5 mV (bipolar) and >5.5 mV (unipolar, free wall).[58,64,67] However, we have shown that unipolar voltage correlating with CMR scar along the posterior RVOT opposite the aortic root tends to be lower than the rest of the posterior septal area, and the authors calculated optimal unipolar voltage cut-off values of 6 mV for the posterior aspect of the RVOT opposite to the aortic root and 7.5 mV for the remainder of the septal aspect of the RV.[68]

Santangeli et al. reported in a mixed cohort of 18 patients with ARVC, 13 patients with myocarditis and five with idiopathic RVOT arrhythmias that the distribution of LGE correlated well with the distribution of EAVM scar defined as bipolar voltage of <1.5 mV, including free wall, posterior/inferior wall as well as RVOT. However,

the existence of LGE on CMR missed 91% of EAVM substrates when the RV EAVM scar area was <20%, indicating that EAVM is much more sensitive for substrate identification than CMRI when the scar burden is low.[69]

Recently, we reported the association of regional LGE-CMR standardised intensity with 3,205 epicardial electrogram map points in 10 ARVC patients. Bipolar (–1.43 mV/z-score; p<0.001) and unipolar voltage amplitude (–1.22 mV/z-score; p<0.001) were associated with regional signal intensity standardised by z-scores. Signal intensity z-score thresholds >0.05 (95% CI [–0.05–0.15]) and <–0.16 (95% CI [–0.26–0.06]) corresponded to bipolar voltage measures <0.5 and >1.0 mV, respectively.[70] The characterisation of different image modalities in association with arrhythmogenic substrates are summarised in *Table 2*.

Innovative Image-guided Treatments

Recently, innovative imaging-guided treatments have been utilised for refractory VT patients. For patients with severe adhesions post cardiac surgery or repeated epicardial ablations limiting standard percutaneous epicardial access, Aksu et al. described a minimally invasive surgical approach to achieve epicardial access via video-assisted thoracoscopy.[71] Stereotactic body radiation therapy (SBRT) is an increasingly utilised non-invasive therapy for patients with refractory VT.

Cuculich et al. performed SBRT in five high-risk refractory VT patients and demonstrated dramatic reduction of VT burden over long-term follow-up.[72] The recent Phase I/II Study of EP-guided Noninvasive Cardiac Radioablation for Treatment of Ventricular Tachycardia (ENCORE-VT), was a single-arm prospective study that demonstrated SBRT to be associated with marked reduction of VT burden, and as such may be a viable alternative treatment option for patients with VT refractory to ablation.[73]

Sympathetic hyperactivity clearly plays a vital role in the genesis and maintenance of ventricular arrhythmias, and cardiac sympathetic denervation has been reported as the effective VT treatment which can reduce the burden of ICD shocks.[74-76] Vaseghi et al. demonstrated that bilateral cardiac sympathetic denervation is more beneficial than left cardiac sympathetic denervation in VT storm patients.[77] Of note, PET imaging can be helpful in assessing cardiac sympathetic innervation.[78]

Limitations of Cardiac Imaging Assessment and Image Integration

Image Resolution and Presence of ICDs

It is challenging to delineate the border zone substrate using partial volume averaging with LGE. Schelbert et al. acquired CMR imaging utilising 7 Telsa scanner to identify post-infarction myocardial fibrosis in the *ex vivo* rat heart and demonstrated that the intermediate signal intensity is resolution dependent.[79] Of note, high resolution images can identify intermediate signal intensity voxels correlating with histological fibrosis and a possible VT isthmus, but blur with normal myocardium when image resolution declines due to partial volume effect.

In patients with pacemakers and ICDs, imaging artifact from the pulse generator and leads can limit the interpretation of substrate from CMR or CT. The application of a wideband LGE sequence has reduced the hyper-enhanced CMR artifact, however, the dark magnetic susceptibility artifacts remain problematic. Additionally, the current 3D in-plane resolution of wideband sequences is limited to 1.5 × 1.5 mm with slice thicknesses ranging from 4–8 mm, which may not be sufficient to clearly delineate critical VT isthmuses.[80,81] One advantage of CT compared with delayed enhancement (DE)-CMR is that device-related artifact can be quantified logically: each voxel with a value >20% of the maximum density can be considered as hyperdense artifacts, while voxels with values less than –150 HU can be considered as hypodense artifacts.[82]

Furthermore, although evolving evidence indicates that CMR can be safely performed in patients with devices, including those who are pacemaker dependent, and even in those with abandoned leads or non-MRI conditional systems,CMR may not be universally offered by all centres for patients with ICDs at the current time.[83,84]

Functional Ventricular Tachycardia Isthmus Assessment

The above-mentioned imaging modalities focus on the detection of structural abnormalities and their association with demonstrated EAVM substrates in non-ischaemic VT patients. Few studies have correlated the imaging detected abnormalities to the functional VT isthmuses in NICM patients.[7]

Anter et al. identified the VT critical isthmus zone, corresponding to the location of a steep activation gradient and very low voltage amplitude during sinus rhythm in the post-infarction swine model.[85] The functional electroanatomical high-density mapping allows identification of VT reentrant circuits whilst the EAVM or electrograms during sinus rhythm have limited specificity to identify VT circuits.

Ciaccio et al. proposed the source-sink mismatch model to explain how the ischaemic VT re-entrant circuits form and become sustained.[86] Of note, it is typically challenging to precisely identify non-ischaemic VT circuits and correlate circuit components with imaging structural abnormalities due to the haemodynamic instability and multiple VT morphologies.

Lack of Evidence Associating Histology and Non-ischaemic Scar Detected by Cardiac MRI or CT

There is no agreement on the optimal method and SI thresholds, as well as CT attenuation thresholds to delineate fibrosis/scar or border zone area within scars validated by histology in the setting of prior infarction. Prior studies have utilised various methods to identify fibrosis/scar on the LGE-CMR and CT angiography. By LGE-CMR, the thresholds can be defined using standardised myocardial SI.

One methodology sets thresholds at 35%, 50% or 40% and 60%[7,28,22] to distinguish scar core and border zone area from normal myocardium. For NICM patients, 6 standard deviations above the average SI of healthy remote myocardium has been utilised to define scar.[18] In CT, scar may be estimated as hypo-attenuation regions on immediate first pass imaging, or as hyper-attenuation regions on DE imaging acquired 10 minutes after contrast agent injection.

Similar to CMR, the extent of scar based upon CT attenuation can be assessed visually or quantitatively using specialised software. Wall thinning <5 mm with LV bulging or aneurysmal dilation can also be used to estimate scar distribution.[24] Compared to CMR, CT offers exceptional spatial resolution. However, CMR offers improved temporal and contrast resolution. The optimal method to identify scar employing

either LGE-CMR or CT imaging remains to be definitively elucidated and will likely depend upon the patient condition, renal function, ability to breath hold, and institutional resources. The current evidence for scar delineation by imaging in NICM is primarily based on the association with electroanatomical mapping and abnormal electrograms.

Conclusion

The underlying VT substrate in patients with NICM can be quite variable, depending on the underlying NICM aetiology. Pre-procedural multimodality imaging and intra-procedural image integration can be helpful to delineate VT substrate and facilitate safe and effective VT ablation in patients with NICM. ■

Clinical Perspective

- The arrhythmogenic substrate can differ, depending on the aetiology of non-ischaemic cardiomyopathy (NICM).
- Multimodality imaging is helpful to characterise the substrate in patients with NICM prior to ventricular tachycardia (VT) ablation.
- Image integration, although not yet characterising detailed histology, can delineate the location and extent of the VT substrate and appears to facilitate safe and effective VT ablation.

1. Muser D, Santangeli P, Castro SA, et al. Long-term outcome after catheter ablation of ventricular tachycardia in patients with nonischemic dilated cardiomyopathy. *Circ Arrhythm Electrophysiol* 2016;9:e004328. https://doi.org/10.1161/CIRCEP.116.004328; PMID: 27733494.
2. Kumar S, Barbhaiya C, Nagashima K, et al. Ventricular tachycardia in cardiac sarcoidosis: characterization of ventricular substrate and outcomes of catheter ablation. *Circ Arrhythm Electrophysiol* 2015;8:87–93. https://doi.org/10.1161/CIRCEP.114.002145; PMID: 25527825.
3. Dinov B, Fiedler L, Schonbauer R, et al. Outcomes in catheter ablation of ventricular tachycardia in dilated nonischemic cardiomyopathy compared with ischemic cardiomyopathy: results from the Prospective Heart Centre of Leipzig VT (HELP-VT) study. *Circulation* 2014;129:728–36. https://doi.org/10.1161/CIRCULATIONAHA.113.003063; PMID: 24211823.
4. Elliott P, Andersson B, Arbustini E, et al. Classification of the cardiomyopathies: a position statement from the European Society of Cardiology Working Group on Myocardial and Pericardial Diseases. *Eur Heart J* 2008;29:270–6. https://doi.org/10.1161/CIRCULATIONAHA.113.003063; PMID: 24211823.
5. Vaseghi M, Hu TY, Tung R, et al. Outcomes of catheter ablation of ventricular tachycardia based on etiology in nonischemic heart disease: an international ventricular tachycardia ablation center collaborative study. *JACC Clin Electrophysiol* 2018;4:1141–50.https://doi.org/10.1016/j.jacep.2018.05.007; PMID: 30236386.
6. Piers SR, Leong DP, van Huls van Taxis CF, et al. Outcome of ventricular tachycardia ablation in patients with nonischemic cardiomyopathy: the impact of noninducibility. *Circ Arrhythm Electrophysiol* 2013;6:513–21. https://doi.org/10.1161/CIRCEP.113.000089; PMID: 23619893.
7. Piers SR, Tao Q, de Riva Silva M, et al. CMR-based identification of critical isthmus sites of ischemic and nonischemic ventricular tachycardia. *JACC Cardiovasc Imaging* 2014;7:774–84. https://doi.org/10.1016/j.jcmg.2014.03.013; PMID: 25051947.
8. Kapelko VI. Extracellular matrix alterations in cardiomyopathy: The possible crucial role in the dilative form. *Exp Clin Cardiol* 2001;6:41–9. PMID: 20428444.
9. Liuba I, Frankel DS, Riley MP, et al. Scar progression in patients with nonischemic cardiomyopathy and ventricular arrhythmias. *Heart Rhythm* 2014;11:755–62. https://doi.org/10.1016/j.hrthm.2014.02.012; PMID: 24561162.
10. Karamitsos TD, Francis JM, Myerson S, et al. The role of cardiovascular magnetic resonance imaging in heart failure. *J Am Coll Cardiol* 2009;54:1407–24. https://doi.org/10.1016/j.jacc.2009.04.094; PMID: 19796734.
11. Tao Q, Piers SR, Lamb HJ, et al. Preprocedural magnetic resonance imaging for image-guided catheter ablation of scar-related ventricular tachycardia. *Int J Cardiovasc Imaging* 2015;31:369–77. https://doi.org/10.1007/s10554-014-0558-x; PMID: 25341408.
12. Gupta S, Desjardins B, Baman T, et al. Delayed-enhanced MR scar imaging and intraprocedural registration into an electroanatomical mapping system in post-infarction patients. *JACC Cardiovasc Imaging* 2012;5:207–10. https://doi.org/10.1016/j.jcmg.2011.08.021; PMID: 22340829.
13. Desjardins B, Crawford T, Good E, et al. Infarct architecture and characteristics on delayed enhanced magnetic resonance imaging and electroanatomic mapping in patients with postinfarction ventricular arrhythmia. *Heart Rhythm* 2009;6:644–51. https://doi.org/10.1016/j.hrthm.2009.02.018; PMID: 19389653.
14. Andreu D, Berruezo A, Ortiz-Perez JT, et al. Integration of 3D electroanatomic maps and magnetic resonance scar characterization into the navigation system to guide ventricular tachycardia ablation. *Circ Arrhythm Electrophysiol* 2011;4:674–83. https://doi.org/10.1161/CIRCEP.111.961946; PMID: 21880674.
15. Ghannam M, Cochet H, Jais P, et al. Correlation between computer tomography-derived scar topography and critical ablation sites in postinfarction ventricular tachycardia. *J Cardiovasc Electrophysiol* 2018;29:438–45. https://doi.org/10.1111/jce.13441; PMID: 29380921.
16. Copie X, Blankoff I, Hnatkova K, et al. Influence of the duration of recording in the reproducibility of the signal averaged electrocardiogram. *Arch Mal Coeur Vaiss* 1996;89:723–7 [in French]. PMID: 8760658.
17. Cedilnik N, Duchateau J, Dubois R, et al. Fast personalized electrophysiological models from computed tomography images for ventricular tachycardia ablation planning. *Europace* 2018;20(Suppl 3):iii94–101. https://doi.org/10.1093/europace/euy228; PMID: 30476056.
18. Sasaki T, Miller CF, Hansford R, et al. Impact of nonischemic scar features on local ventricular electrograms and scar-related ventricular tachycardia circuits in patients with nonischemic cardiomyopathy. *Circ Arrhythm Electrophysiol* 2013;6:1139–47. https://doi.org/10.1161/CIRCEP.113.000159; PMID: 24235267.
19. Bogun FM, Desjardins B, Good E, et al. Delayed-enhanced magnetic resonance imaging in nonischemic cardiomyopathy: utility for identifying the ventricular arrhythmia substrate. *J Am Coll Cardiol* 2009;53:1138–45. https://doi.org/10.1016/j.jacc.2008.11.052; PMID: 19324259.
20. Yamashita S, Sacher F, Mahida S, et al. Role of high-resolution image integration to visualize left phrenic nerve and coronary arteries during epicardial ventricular tachycardia ablation. *Circ Arrhythm Electrophysiol* 2015;8:371–80. https://doi.org/10.1161/CIRCEP.114.002420; PMID: 25713213.
21. Yamashita S, Sacher F, Mahida S, et al. Image integration to guide catheter ablation in scar-related ventricular tachycardia. *J Cardiovasc Electrophysiol.* 2016;27:699–708. https://doi.org/10.1111/jce.12963; PMID: 26918883.
22. Andreu D, Ortiz-Perez JT, Fernandez-Armenta J, et al. 3D delayed-enhanced magnetic resonance sequences improve conducting channel delineation prior to ventricular tachycardia ablation. *Europace* 2015;17:938–45. https://doi.org/10.1093/europace/euu310; PMID: 25616406.
23. Siontis KC, Kim HM, Sharaf Dabbagh G, et al. Association of preprocedural cardiac magnetic resonance imaging with outcomes of ventricular tachycardia ablation in patients with idiopathic dilated cardiomyopathy. *Heart Rhythm* 2017;14:1487–93. https://doi.org/10.1016/j.hrthm.2017.06.003; PMID: 28603002.
24. Esposito A, Palmisano A, Antunes S, et al. Cardiac CT with delayed enhancement in the characterization of ventricular tachycardia structural substrate: relationship between CT-segmented scar and electro-anatomic mapping. *JACC Cardiovasc Imaging* 2016;9:822–32. https://doi.org/10.1016/j.jcmg.2015.10.024; PMID: 26897692.
25. Piers SR, van Huls van Taxis CF, Tao Q, et al. Epicardial substrate mapping for ventricular tachycardia ablation in patients with non-ischaemic cardiomyopathy: a new algorithm to differentiate between scar and viable myocardium developed by simultaneous integration of computed tomography and contrast-enhanced magnetic resonance imaging. *Eur Heart J* 2013;34:586–96. https://doi.org/10.1093/eurheartj/ehs382; PMID: 23161702.
26. Hsia HH, Callans DJ, Marchlinski FE. Characterization of endocardial electrophysiological substrate in patients with nonischemic cardiomyopathy and monomorphic ventricular tachycardia. *Circulation* 2003;108:704–10. https://doi.org/10.1161/01.CIR.0000083725.72693.EA; PMID: 12885746.
27. Oloriz T, Silberbauer J, Maccabelli G, et al. Catheter ablation of ventricular arrhythmia in nonischemic cardiomyopathy: anteroseptal versus inferolateral scar sub-types. *Circ Arrhythm Electrophysiol* 2014;7:414–23. https://doi.org/10.1161/CIRCEP.114.001568; PMID: 24785410.
28. Piers SR, Tao Q, van Huls van Taxis CF, et al. Contrast-enhanced MRI-derived scar patterns and associated ventricular tachycardias in nonischemic cardiomyopathy: implications for the ablation strategy. *Circ Arrhythm Electrophysiol* 2013;6:875–83. https://doi.org/10.1161/CIRCEP.113.000537; PMID: 24036134.
29. Tung R, Bauer B, Schelbert H, et al. Incidence of abnormal positron emission tomography in patients with unexplained cardiomyopathy and ventricular arrhythmias: The potential role of occult inflammation in arrhythmogenesis. *Heart Rhythm* 2015;12:2488–98. https://doi.org/10.1016/j.hrthm.2015.08.014; PMID: 26272522.
30. Bauer BS, Li A, Bradfield JS. arrhythmogenic inflammatory cardiomyopathy: a review. *Arrhythm Electrophysiol Rev* 2018;7:181–6. https://doi.org/10.15420/aer.2018.26.2; PMID: 30416731.
31. Orii M, Imanishi T, Akasaka T. Assessment of cardiac sarcoidosis with advanced imaging modalities. *Biomed Res Int* 2014;2014:897956. https://doi.org/10.1155/2014/897956; PMID: 25250336.
32. Ohira H, Tsujino I, Ishimaru S, et al. Myocardial imaging with 18F-fluoro-2-deoxyglucose positron emission tomography and magnetic resonance imaging in sarcoidosis. *Eur J Nucl Med Mol Imaging* 2008;35:933–41. https://doi.org/10.1007/s00259-007-0650-8; PMID: 18084757.
33. Chareonthaitawee P, Beanlands RS, Chen W, et al. Joint SNMMI-ASNC expert consensus document on the role of (18)F-FDG PET/CT in cardiac sarcoid detection and therapy monitoring. *J Nucl Med* 2017;58:1341–53. https://doi.org/10.2967/jnumed.117.196287; PMID: 28765228.
34. Patel MR, Cawley PJ, Heitner JF, et al. Detection of myocardial damage in patients with sarcoidosis. *Circulation* 2009;120:1969–77. https://doi.org/10.1161/CIRCULATIONAHA.109.851352; PMID: 19884472.
35. Smedema JP, Snoep G, van Kroonenburgh MP, et al. Evaluation of the accuracy of gadolinium-enhanced cardiovascular magnetic resonance in the diagnosis of cardiac sarcoidosis. *J Am Coll Cardiol* 2005;45:1683–90. https://doi.org/10.1016/j.jacc.2005.01.047; PMID: 15893188.
36. Ichinose A, Otani H, Oikawa M, et al. MRI of cardiac sarcoidosis: basal and subepicardial localization of myocardial lesions and their effect on left ventricular function. *AJR Am J Roentgenol* 2008;191:862–9. https://doi.org/10.2214/AJR.07.3089; PMID: 18716120.
37. Muser D, Santangeli P, Liang JJ, et al. Characterization of the electroanatomic substrate in cardiac sarcoidosis: correlation with imaging findings of scar and inflammation. *JACC Clin Electrophysiol* 2018;4:291–303. https://doi.org/10.1016/j.jacep.2017.09.175; PMID: 30089553.
38. Shirani J, Roberts WC. Subepicardial myocardial lesions. *Am Heart J* 1993;125:1346–52. https://doi.org/10.1016/0002-8703(93)91005-Y; PMID: 8480587.
39. Tavora F, Cresswell N, Li L, et al. Comparison of necropsy findings in patients with sarcoidosis dying suddenly from cardiac sarcoidosis versus dying suddenly from other causes. *Am J Cardiol* 2009;104:571–7. https://doi.org/10.1016/j.amjcard.2009.03.068; PMID: 19660614.
40. Blankstein R, Osborne M, Naya M, et al. Cardiac positron emission tomography enhances prognostic assessments of patients with suspected cardiac sarcoidosis. *J Am Coll Cardiol* 2014;63:329–36. https://doi.org/10.1016/j.jacc.2013.09.022; PMID: 24140661.
41. Yalagudri S, Zin Thu N, Devidutta S, et al. Tailored approach for management of ventricular tachycardia in cardiac sarcoidosis. *J Cardiovasc Electrophysiol* 2017;28:893–902. https://doi.org/10.1111/jce.13228; PMID: 28429512.
42. Papageorgiou N, Providencia R, Bronis K, et al. Catheter ablation for ventricular tachycardia in patients with cardiac sarcoidosis: a systematic review. *Europace* 2018;20:682–91. https://doi.org/10.1093/europace/eux077; PMID: 28444174.
43. Holmstrom M, Kivisto S, Helio T, et al. Late gadolinium enhanced cardiovascular magnetic resonance of lamin A/C gene mutation related dilated cardiomyopathy. *J Cardiovasc Magn Reson* 2011;13:30. https://doi.org/10.1186/1532-429X-13-30; PMID: 21689390.
44. Kumar S, Androulakis AF, Sellal JM, et al. Multicenter experience with catheter ablation for ventricular tachycardia in lamin A/C cardiomyopathy. *Circ Arrhythm Electrophysiol* 2016;9:e004357. https://doi.org/10.1161/CIRCEP.116.004357; PMID: 27506821.
45. Friedrich MG, Sechtem U, Schulz-Menger J, et al. Cardiovascular magnetic resonance in myocarditis: a JACC white paper. *J Am Coll Cardiol* 2009;53:1475–87. https://doi.org/10.1016/j.jacc.2009.02.007; PMID: 19389557.
46. Maccabelli G, Tsiachris D, Silberbauer J, et al. Imaging and epicardial substrate ablation of ventricular tachycardia in patients late after myocarditis. *Europace* 2014;16:1363–72. https://doi.org/10.1093/europace/euu017; PMID: 24558183.
47. Reithmann C, Herkommer B, Fiek M. Epicardial ventricular tachycardia substrate visualized by magnetic resonance imaging: need for a transpericardial ablation approach? *Clin Res Cardiol* 2016;105:827–37. https://doi.org/10.1007/s00392-016-0990-0; PMID: 27294860.

48. Maron BJ, Towbin JA, Thiene G, et al. Contemporary definitions and classification of the cardiomyopathies: an American Heart Association Scientific Statement from the Council on Clinical Cardiology, Heart Failure and Transplantation Committee; Quality of Care and Outcomes Research and Functional Genomics and Translational Biology Interdisciplinary Working Groups; and Council on Epidemiology and Prevention. *Circulation* 2006;113:1807–16. https://doi.org/10.1161/CIRCULATIONAHA.106.174287; PMID: 16567565.
49. Jenni R, Oechslin E, Schneider J, et al. Echocardiographic and pathoanatomical characteristics of isolated left ventricular non-compaction: a step towards classification as a distinct cardiomyopathy. *Heart* 2001;86:666–71. http://dx.doi.org/10.1136/heart.86.6.666; PMID: 11711464.
50. Muser D, Nucifora G, Gianfagna E, et al. Clinical spectrum of isolated left ventricular noncompaction: thromboembolic events, malignant left ventricular arrhythmias, and refractory heart failure. *J Am Coll Cardiol* 2014;63:e39. https://doi.org/10.1016/j.jacc.2013.11.063; PMID: 24576431.
51. Oechslin EN, Attenhofer Jost CH, Rojas JR, et al. Long-term follow-up of 34 adults with isolated left ventricular noncompaction: a distinct cardiomyopathy with poor prognosis. *J Am Coll Cardiol* 2000;36:493–500; https://doi.org/10.1016/S0735-1097(00)00755-5; PMID: 10933363.
52. Muser D, Liang JJ, Witschey WR, et al. Ventricular arrhythmias associated with left ventricular noncompaction: Electrophysiologic characteristics, mapping, and ablation. *Heart Rhythm* 2017;14:166–75. https://doi.org/10.1016/j.hrthm.2016.11.014; PMID: 27890738.
53. Wan J, Zhao S, Cheng H, et al. Varied distributions of late gadolinium enhancement found among patients meeting cardiovascular magnetic resonance criteria for isolated left ventricular non-compaction. *J Cardiovasc Magn Reson* 2013;15:20. https://doi.org/10.1186/1532-429X-15-20; PMID: 23421977.
54. Akdis D, Brunckhorst C, Duru F, Saguner AM. Arrhythmogenic cardiomyopathy: electrical and structural phenotypes. *Arrhythm Electrophysiol Rev* 2016;5:90–101. https://doi.org/10.15420/AER.2016.4.3; PMID: 27617087.
55. Riley MP, Zado E, Bala R, et al. Lack of uniform progression of endocardial scar in patients with arrhythmogenic right ventricular dysplasia/cardiomyopathy and ventricular tachycardia. *Circ Arrhythm Electrophysiol* 2010;3:332–8. https://doi.org/10.1161/CIRCEP.109.919530; PMID: 20558846.
56. Basso C, Corrado D, Marcus FI, et al. Arrhythmogenic right ventricular cardiomyopathy. *Lancet* 2009;373:1289–300. https://doi.org/10.1016/S0140-6736(09)60256-7; PMID: 19362677.
57. Komatsu Y, Jadidi A, Sacher F, et al. Relationship between MDCT-imaged myocardial fat and ventricular tachycardia substrate in arrhythmogenic right ventricular cardiomyopathy. *J Am Heart Assoc* 2014;3:e000935. https://doi.org/10.1161/JAHA.114.000935; PMID: 25103203.
58. Cassidy DM, Vassallo JA, Marchlinski FE, et al. Endocardial mapping in humans in sinus rhythm with normal left ventricles: activation patterns and characteristics of electrograms. *Circulation* 1984;70:37–42. https://doi.org/10.1161/01.CIR.70.1.37; PMID: 6723010.
59. Cano O, Hutchinson M, Lin D, et al. Electroanatomic substrate and ablation outcome for suspected epicardial ventricular tachycardia in left ventricular nonischemic cardiomyopathy. *J Am Coll Cardiol* 2009;54:799–808. https://doi.org/10.1016/j.jacc.2009.05.032; PMID: 19695457.
60. Desjardins B, Yokokawa M, Good E, et al. Characteristics of intramural scar in patients with nonischemic cardiomyopathy and relation to intramural ventricular arrhythmias. *Circ Arrhythm Electrophysiol* 2013;6:891–7. https://doi.org/10.1161/CIRCEP.113.000073; PMID: 23985383.
61. Liang JJ, D'Souza BA, Betensky BP, et al. Importance of the interventricular septum as part of the ventricular tachycardia substrate in nonischemic cardiomyopathy. *JACC Clin Electrophysiol* 2018;4:1155–62. https://doi.org/10.1016/j.jacep.2018.04.016; PMID: 30236388.
62. Cochet H, Komatsu Y, Sacher F, et al. Integration of merged delayed-enhanced magnetic resonance imaging and multidetector computed tomography for the guidance of ventricular tachycardia ablation: a pilot study. *J Cardiovasc Electrophysiol* 2013;24:419–26. https://doi.org/10.1111/jce.12052; PMID: 23252727.
63. Bazan V, Santangeli P, Marchlinski FE. Using endocardial unipolar mapping to identify epicardial scar: When and how to adjust the voltage amplitude slider bar? *Pacing Clin Electrophysiol* 2018;41:342–4; https://doi.org/10.1111/pace.13298; PMID: 29430667.
64. Hutchinson MD, Gerstenfeld EP, Desjardins B, et al. Endocardial unipolar voltage mapping to detect epicardial ventricular tachycardia substrate in patients with nonischemic left ventricular cardiomyopathy. *Circ Arrhythm Electrophysiol* 2011;4:49–55. https://doi.org/10.1161/CIRCEP.110.959957; PMID: 21131557.
65. Santangeli P, Marchlinski FE. Substrate mapping for unstable ventricular tachycardia. *Heart Rhythm* 2016;13:569–83. https://doi.org/10.1016/j.hrthm.2015.09.023; PMID: 26410105.
66. Glashan CA, Androulakis AFA, Tao Q, et al. Whole human heart histology to validate electroanatomical voltage mapping in patients with non-ischaemic cardiomyopathy and ventricular tachycardia. *Eur Heart J* 2018;39:2867–75. https://doi.org/10.1093/eurheartj/ehy168; PMID: 29617764.
67. Polin GM, Haqqani H, Tzou W, et al. Endocardial unipolar voltage mapping to identify epicardial substrate in arrhythmogenic right ventricular cardiomyopathy/dysplasia. *Heart Rhythm* 2011;8:76–83. https://doi.org/10.1016/j.hrthm.2010.09.088; PMID: 20933099.
68. Kelesidis I, Desjardins B, Muser D, et al. Unipolar voltage mapping criteria for right ventricular septum: Influence of the aortic root. *J Cardiovasc Electrophysiol* 2018;29:1113–8. https://doi.org/10.1111/jce.13630; PMID: 29727513.
69. Santangeli P, Hamilton-Craig C, Dello Russo A, et al. Imaging of scar in patients with ventricular arrhythmias of right ventricular origin: cardiac magnetic resonance versus electroanatomic mapping. *J Cardiovasc Electrophysiol* 2011;22:1359–66. https://doi.org/10.1111/j.1540-8167.2011.02127.x; PMID: 21736658.
70. Xie S, Desjardins B, Kubala M, et al. Association of regional epicardial right ventricular electrogram voltage amplitude and late gadolinium enhancement distribution on cardiac magnetic resonance in patients with arrhythmogenic right ventricular cardiomyopathy: implications for ventricular tachycardia ablation. *Heart Rhythm* 2018;15:987–93. https://doi.org/10.1016/j.hrthm.2018.02.030; PMID: 29501666.
71. Aksu T, Erdem Guler T, Yalin K. Successful ablation of an epicardial ventricular tachycardia by video-assisted thoracoscopy. *Europace* 2015;17:1116. https://doi.org/10.1093/europace/euv012; PMID: 25736561.
72. Cuculich PS, Schill MR, Kashani R, et al. Noninvasive cardiac radiation for ablation of ventricular tachycardia. *N Engl J Med* 2017;377:2325–36. https://doi.org/10.1056/NEJMoa1613773; PMID: 29236642.
73. Robinson CG, Samson PP, Moore KMS, et al. Phase I/II trial of electrophysiology-guided noninvasive cardiac radioablation for ventricular tachycardia. *Circulation* 2019;139:313–21. https://doi.org/10.1161/CIRCULATIONAHA.118.038261; PMID: 30586734.
74. Zipes DP, Rubart M. Neural modulation of cardiac arrhythmias and sudden cardiac death. *Heart Rhythm* 2006;3:108–13. https://doi.org/10.1016/j.hrthm.2005.09.021; PMID: 16399065.
75. Vaseghi M, Shivkumar K. The role of the autonomic nervous system in sudden cardiac death. *Prog Cardiovasc Dis* 2008;50:404–19. https://doi.org/10.1016/j.pcad.2008.01.003; PMID: 18474284.
76. Vaseghi M, Barwad P, Malavassi Corrales FJ, et al. Cardiac sympathetic denervation for refractory ventricular arrhythmias. *J Am Coll Cardiol* 2017;69:3070–80. https://doi.org/10.1016/j.jacc.2017.04.035; PMID: 28641796.
77. Vaseghi M, Gima J, Kanaan C, et al. Cardiac sympathetic denervation in patients with refractory ventricular arrhythmias or electrical storm: intermediate and long-term follow-up. *Heart Rhythm* 2014;11:360–6. https://doi.org/10.1016/j.hrthm.2013.11.028; PMID: 24291775.
78. Sasano T, Abraham MR, Chang KC, et al. Abnormal sympathetic innervation of viable myocardium and the substrate of ventricular tachycardia after myocardial infarction. *J Am Coll Cardiol* 2008;51:2266–75. https://doi.org/10.1016/j.jacc.2008.02.062; PMID: 18534275.
79. Schelbert EB, Hsu LY, Anderson SA, et al. Late gadolinium-enhancement cardiac magnetic resonance identifies postinfarction myocardial fibrosis and the border zone at the near cellular level in ex vivo rat heart. *Circ Cardiovasc Imaging* 2010;3:743–52. https://doi.org/10.1161/CIRCIMAGING.108.835793; PMID: 20847191.
80. Ranjan R, McGann CJ, Jeong EK, et al. Wideband late gadolinium enhanced magnetic resonance imaging for imaging myocardial scar without image artefacts induced by implantable cardioverter-defibrillator: a feasibility study at 3 T. *Europace* 2015;17:483–8. https://doi.org/10.1093/europace/euu263; PMID: 25336666.
81. Rashid S, Rapacchi S, Shivkumar K, et al. Modified wideband three-dimensional late gadolinium enhancement MRI for patients with implantable cardiac devices. *Magn Reson Med* 2016;75:572–84. https://doi.org/10.1002/mrm.25601; PMID: 25772155.
82. Prell D, Kalender WA, Kyriakou Y. Development, implementation and evaluation of a dedicated metal artefact reduction method for interventional flat-detector CT. *Br J Radiol* 2010;83:1052–62. https://doi.org/10.1259/bjr/19113084; PMID: 20858662.
83. Nazarian S, Hansford R, Rahsepar AA, et al. Safety of magnetic resonance imaging in patients with cardiac devices. *N Engl J Med* 2017;377:2555–64. https://doi.org/10.1056/NEJMoa1604267; PMID: 29281579.
84. Russo RJ, Costa HS, Silva PD, et al. Assessing the risks associated with MRI in patients with a pacemaker or defibrillator. *N Engl J Med* 2017;376:755–64. https://doi.org/10.1056/NEJMoa1603265; PMID: 28225684.
85. Anter E, Kleber AG, Rottmann M, et al. Infarct-related ventricular tachycardia: redefining the electrophysiological substrate of the isthmus during sinus rhythm. *JACC Clin Electrophysiol* 2018;4:1033–48. https://doi.org/10.1016/j.jacep.2018.04.007; PMID: 30139485.
86. Ciaccio EJ, Coromilas J, Wit AL, et al. Source-sink mismatch causing functional conduction block in re-entrant ventricular tachycardia. *JACC Clin Electrophysiol* 2018;4:1–16. https://doi.org/10.1016/j.jacep.2017.08.019; PMID: 29600773.
87. Spears DA, Suszko AM, Dalvi R, et al. Relationship of bipolar and unipolar electrogram voltage to scar transmurality and composition derived by magnetic resonance imaging in patients with nonischemic cardiomyopathy undergoing VT ablation. *Heart Rhythm* 2012;9:1837–46. https://doi.org/10.1016/j.hrthm.2012.07.022; PMID: 22846338.
88. Dickfeld T, Lei P, Dilsizian V, et al. Integration of three-dimensional scar maps for ventricular tachycardia ablation with positron emission tomography-computed tomography. *JACC Cardiovasc Imaging* 2008;1:73–82. https://doi.org/10.1016/j.jcmg.2007.10.001; PMID: 19356409.